J Fluoresc (2012) 22:865–870
DOI 10.1007/s10895-011-1023-z

ORIGINAL PAPER

Universal Correlation Between Solvent Polarity, Fluorescence Lifetime and Macroscopic Viscosity of Alcohol Solutions

Pradip Kumar · H. B. Bohidar

Received: 11 October 2011 / Accepted: 29 November 2011 / Published online: 12 January 2012

Abstract In this report, we show interesting correlation between solvent polarity of alcohol solutions and fluorescence lifetime (τ_{av}), estimated from time-resolved fluorescence spectroscopy (TRFS), and macroscopic viscosity (η). Non-functionalized carbon nanoparticles (NCNP) were successfully used as flurophores in these measurements. The solvent polarity, described through polarizability (Δf) of dielectric continuum theory, could universally describe both τ_{av}/τ_{max} and η/η_{max} through the relation, $X(\Delta f) = a_{OH} + b(\Delta f - \Delta f_{OH}) + c(\Delta f - \Delta f_{OH})^2$ with X = τ_{av}/τ_{max} or η/η_{max}, (subscript OH represents corresponding values for alcohols) for alcohol solutions of methanol, ethanol and 1-propanol at room temperature. We show that fluorescence lifetime and solvent viscosity are universal functions of solvent polarity for alcohol solutions.

Keywords Solvent polarity · Viscosity · Carbon nanoparticles · Fluorescence lifetime

Introduction

Study of physical properties of water-alcohol system has generated considerable interest in the past because of the unique liquid-liquid phase equilibria exhibited by these liquids. Particularly, methanol, ethanol and 1-propanol are miscible with water in all proportions. The mixing curve depicts one universal feature; that is, all these alcohols show maximum viscosity and refractive index when the alcohol mole fraction, $x \approx 0.3$. It has been established in the past that maximum hydrogen bonding between alcohol and water molecules occurs at this composition. Modeling the hydrophobic effect remains a challenge. However, it is relatively easier to study model hydrophobic systems from an experimental perspective. A common method of investigation of systems where the role of solvent hydrophobicity can determine the nature and extent of interactions is to alter the water structure by adding small quantities of monohydric alcohols of different chain lengths [1, 2]. Such alcohol solutions have been studied extensively [3–6]. Dilute aqueous solutions of monohydric alcohols can be classified as 'hydrophobic systems' even though alcohol molecules are hetero functional (these have both solvophobic and solvophilic groups). Mixing of water with simple alcohols result in cross intermolecular associations and deviations from ideal thermodynamic mixing behavior have been observed [7, 8]. Binary mixed solvents has been extensively used as media for carrying out physico-chemical investigations of organic molecules [9, 10], to assess the formation and stabilization of twisted intermolecular charge transfer states [11, 12].

A change in the microscopic environment of the solvent has profound effect on its fluorescence properties that owes its origin to change in polarity, dielectric constant, polarizability etc. These parameters can easily altered by mixing the two solvents in different proportions. The fluorescence property strongly depends on the immediate environment of the fluorophore. The excited state lifetime of the fluorophore is a parameter that is very sensitive to the local environment. Therefore a systematic analysis of binary solvents effects is informative and proves useful in studying the excited state behavior of the fluorophore. In this study, three hydrogen bond–donating solvents (primary alcohols) were chosen as model dispersion media. These were mixed with water to

P. Kumar · H. B. Bohidar (✉)
Nanomaterials and Nanocomposites Laboratory,
School of Physical Sciences, Jawaharlal Nehru University,
New Delhi 110067, India
e-mail: bohi0700@mail.jnu.ac.in

generate alcohol solutions of desired alcohol concentration. Thus, by changing alcohol mole fraction (χ_{OH}), it is possible to control the solvent polarity (hydrophobicity), viscosity, refractive index and dielectric constant. When alcohol concentration is raised, the physical properties (refractive index, dielectric constant, viscosity) and hence polarity of the water–alcohol binary mixture is continuously changed. Polarity is reduced and its hydrophobicity is increased. In this work, we have used non-functionalized carbon nanoparticles as fluorphores and measure average fluorescence lifetime to correlate this parameter with solution viscosity. Aqueous solutions limited to three primary alcohols, methanol, ethanol and 1-propanol, were chosen as model solvents. Higher alcohols were immiscible with water. We show that fluorescence lifetime and solvent viscosity are universal function of solvent polarity.

Experimental Details

All solvents examined in this study were spectroscopic grade (purity 99.9%) obtained from Merck and used as received. The carbon nanoparticles were prepared from lamp soot which is broadly described in our previous work [13, 14] and the exact protocol is provided elsewhere [15]. Typically, 0.1% (w/v) of carbon powder material was dispersed in different ratio of water-alcohols to get the required stock dispersions. These dispersions were stirred with a magnetic stirrer for 6 h to make these homogeneous. The dispersions were allowed to stand for overnight to enable the larger particles and clusters to sediment, and settle at the bottom. This generated optically clear and stable dispersions and was stored in air tight ultra-clean borosilicate glass bottles for future use. All the sample preparations and measurements were carried out at room temperature (25 °C, and RH <50%).

Steady-state absorption and PL emission spectra were recorded using a Cecil CE-7200 (Cecil Instruments, UK) UV–vis spectrophotometer and Varian Cary Eclipse fluorescence spectrometer, respectively. The lifetime decay experiments were performed using time-correlated single photon counting (TCSPC) setup (FL920, Edinburgh Instrument). All samples were excited with diode lasers and the decays were collected at magic angle polarization (55^0). Further details about TRFS and its data analysis can be found elsewhere [16]. Here, we have used picosecond TRFS to probe the solvent effect on the lifetime of relaxations. All the measurements have been done with 100 nm TAC (Time to Amplitude Convertor) at an excitation wavelength of 405 nm. The time resolution for TCSPC setup was~ 120 ps (measured with LUDOX solution). All the emission decays were collected at emission peak wavelengths 460 nm and the data were fitted best to the triple-exponential fitting function (goodness-of-fit (χ^2) values are given in Tables) given by

$$F(t) = a_0 + a1\exp(-t/\tau 1) + a2\exp(-t/\tau 2) + a3\exp(-t/\tau 3) \quad (1)$$

where a_0 is time shift between IRF (Instrument Response Function) and sample decay. τ_1, τ_2, and τ_3 are different component of lifetime correspond to various lifetimes of characteristic excited states with a_1, a_2 and a_3 amplitude, respectively. F(t) could not be fitted either to a single or double exponential function. The average time constant or correlation time is given as

$$\tau_{av} = \langle\tau\rangle = \sum_i a_i\tau_i / \sum_i a_i \quad (2)$$

Results and Discussion

A variety of environmental factors affect fluorescence emission, including interactions between surrounding solvent molecules (dictated by solvent polarity) and the fluorophore, temperature, pH, and the localized concentration of the fluorescent species. The effects of these parameters vary widely from one fluorophore to another, but the absorption and emission spectra can be heavily influenced by environmental variables. In fact, the high degree of sensitivity in fluorescence is primarily due to interactions that occur in the local environment during the excited state lifetime. The general description for environmental effects is given by dielectric continuum theory [17, 18]. This theory mainly assumes that a point dipole solute interacts with the solvent by virtue of the change in solute dipole moment and described by the Lippert-Mataga equation [19, 20].

$$\nu_A - \nu_F = \frac{2}{hc}\left(\frac{\varepsilon-1}{2\varepsilon+1} - \frac{n^2-1}{2n^2+1}\right)\frac{(\mu_E-\mu_G)^2}{a^3} + const \quad (3)$$

Where h is planck's constant, c is the speed of light and a is the radius of cavity in which the fluorophore resides. ν_A and ν_F are the wavenumbers (cm^{-1}) of the absorption and emission, respectively. The interactions responsible for general solvent effects are best understood by derivation of the Lippert equation and can be written as

$$hc\Delta\nu = hc(\nu_A - \nu_F) = \frac{2\Delta f}{a^3}(\mu_E - \mu_G)^2 + const \quad (4)$$

Where $\Delta\nu$ is the frequency shift (in cm^{-1}) between absorption and emission, μ_E and μ_G are the excited and ground state dipole moments, respectively. The term Δf called as orientation polarizability and is described as

$$\Delta f = f(\varepsilon) - f(n) = \frac{\varepsilon-1}{2\varepsilon+1} - \frac{n^2-1}{2n^2+1} \quad (5)$$

Where $f(\varepsilon)$ and $f(n)$ are known as low and high frequency polarizability of molecules.

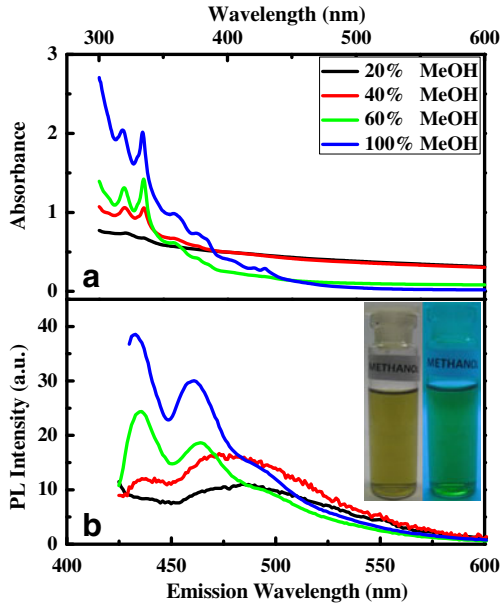

Fig. 1 (**a**) UV–vis absorption spectra, and (**b**) PL spectra (λ_{ex}= 405 nm) for methanol solutions at room temperature. Insert shows photographs of the NCNP dispersion (in methanol) taken under a visible (left) and UV light (right), respectively

Steady State UV and Photoluminescence Spectroscopy

In order to set the experimental protocol some ancillary steady state UV and photoluminescence studies were performed. Spectra (Fig. 1a) have absorption peaks located at 430, 405, 385, 360, 335 and 320 nm. Similar absorption spectra were recorded in case of ethanol and 1-propanol solutions (data are not shown). There was no significant change in the position of the observed absorption bands up to χ_{OH}=1 though peak intensity increased with alcohol concentration. Size heterogeneity present in NCNP could be the main reason behind the origin of multiple absorption bands. It was earlier reported that absorption spectra of NCNP in pure water, showed only absorption bands at 224 and 240 nm [7]. The absorption band at 217 nm is attributed to π-π* band transition in small graphitic or amorphous carbon grains whereas the absorbance band seen around 216–225 nm was argued to be originating from the physical size of the graphitic structure [21]. De Heer and Ugarte observed the 264 nm absorption band in aqueous dispersion of carbon soot [22]. The spectral signature seen in Fig. 1a, implied that the absorption spectra were strongly affected by medium polarizability and viscosity.

Representative spectra for methanol solutions recorded at an excitation wavelength of 405 nm is shown in Fig. 1b. PL emission peaks located at 430 and 460 nm did not change up to 50% alcohol concentration either with solvent polarizability or viscosity in all the three alcohol solutions (data not shown for ethanol and propanol solutions). But, emission peak located at 460 nm was observed to get broader and got red shifted in all alcohol solutions which was clearly observed at 40% alcohol concentration in methanol and ethanol solutions. In case of propanol the corresponding red shift and broadening was observed at 20% alcohol concentration which can be attributed to higher hydrophobicity. The hydrophobicity order in above-mentioned alcohols follows: propanol > ethanol > methanol. Apart from the 460 nm PL peak shifting and broadening, we observed that relative intensity of 430 nm PL peak decreased in comparison to 460 nm PL peak, and it almost disappeared at 20% alcohol solution in all three cases. The optical images of NCNP dispersions (shown only for methanol) under white light and UV exposure (short wavelength) are shown in the inset of Fig. 1b. The bright colors of optical images clearly reveal the fluorescent nature of nanoparticles in methanol.

The origin of red shift in PL spectra and the presence of multiple peaks in the emission spectra could be arising from size heterogeneity of the nanoparticles and/or due to the presence of emissive trap states. All UV–vis and PL experimental results presented above suggest that surrounding medium strongly affect the fluorescence properties of the carbon nanoparticles.

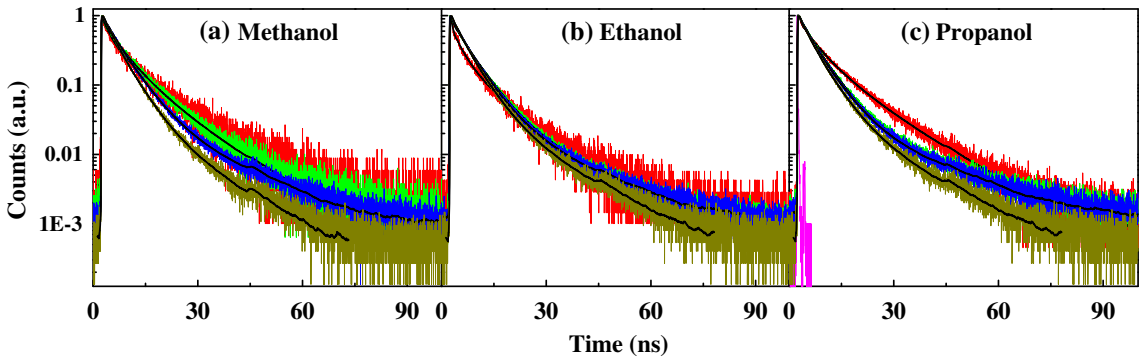

Fig. 2 Time resolved fluorescence decay of NCNP dispersion made in (**a**) water–methanol, (**b**) water-ethanol and (**c**) water-1-propanol mixtures. The red, green, blue and dark yellow lines shown decays in 20, 40, 60 and 100% (v/v) alcohol solutions. All the decays were analyzed with three component fitting model and shown in black lines. The decay shown in pink color represents the IRF

Table 1 Fluorescence decay fitted parameters for NCNP in water-alcohols (water–methanol, water-ethanol and water-1-propanol) solutions

Alcohol% (v/v)	20	30	40	50	60	70	80	90	100
$\chi_{Methanol}$	0.099	0.159	0.228	0.307	0.399	0.508	0.639	0.799	1
χ^2	1.06	1.13	1.09	1.08	1.15	1.13	1.08	1.13	1.10
a_1	0.48	0.33	0.34	0.20	0.19	0.19	0.13	0.19	0.07
τ_1/ns	0.49	0.36	0.44	1.30	1.19	1.40	1.92	1.43	1.11
a_2	0.33	0.37	0.46	0.75	0.76	0.76	0.82	0.76	0.85
τ_2/ns	2.97	3.14	4.75	5.03	5.18	5.07	4.83	5.00	4.07
a_3	0.18	0.28	0.19	0.04	0.05	0.04	0.04	0.04	0.07
τ_3/ns	10.13	10.88	11.97	18.51	17.31	16.14	14.05	15.84	9.83
τ_{av}/ns	3.09	4.43	4.69	4.88	4.98	4.91	4.88	4.79	4.23
$\chi_{Ethanol}$	0.071	0.11	0.17	0.23	0.31	0.41	0.55	0.73	1
χ^2	1.19	1.30	1.12	1.06	1.26	1.05	1.05	1.16	1.07
a_1	0.33	0.27	0.12	0.20	0.33	0.22	0.23	0.22	0.16
τ_1/ns	0.19	0.55	1.36	1.49	1.13	1.44	1.25	1.15	1.13
a_2	0.46	0.66	0.82	0.74	0.52	0.72	0.72	0.73	0.78
τ_2/ns	2.95	5.09	4.52	5.11	5.12	4.96	4.85	4.71	4.27
a_3	0.21	0.06	0.05	0.05	0.14	0.05	0.04	0.04	0.06
τ_3/ns	12.49	15.18	14.59	16.65	12.79	15.88	16.35	15.70	11.45
τ_{av}/ns	4.04	4.45	4.62	5.00	4.90	4.72	4.46	4.44	4.20
$\chi_{Propanol}$	0.0554	0.0914	0.135	0.19	0.26	0.35	0.48	0.67	1
χ^2	1.15	1.20	1.06	1.08	1.07	1.04	1.13	1.14	1.05
a_1	0.27	0.27	0.21	0.20	0.21	0.21	0.22	0.12	0.19
τ_1/ns	0.57	0.30	1.13	1.28	1.51	1.41	1.37	1.32	1.20
a_2	0.65	0.64	0.74	0.75	0.74	0.73	0.72	0.74	0.74
τ_2/ns	5.12	5.12	5.12	5.02	5.04	4.97	4.88	4.72	4.42
a_3	0.07	0.08	0.04	0.04	0.04	0.04	0.05	0.05	0.06
τ_3/ns	14.72	17.04	18.76	18.37	18.34	18.13	16.93	15.66	12.88
τ_{av}/ns	4.61	4.80	4.89	4.88	4.90	4.81	4.70	4.62	4.35

Time Resolved Fluorescence Spectroscopy

The fluorescence decay plots recorded for various alcohol solutions is shown in Fig. 2. The decay curves clearly show that solvent composition (micro-environment) strongly influenced the fluorescence lifetime of NCNP. These curves could not be fitted to single or double exponential decay functions. Thus, needed three lifetime components for

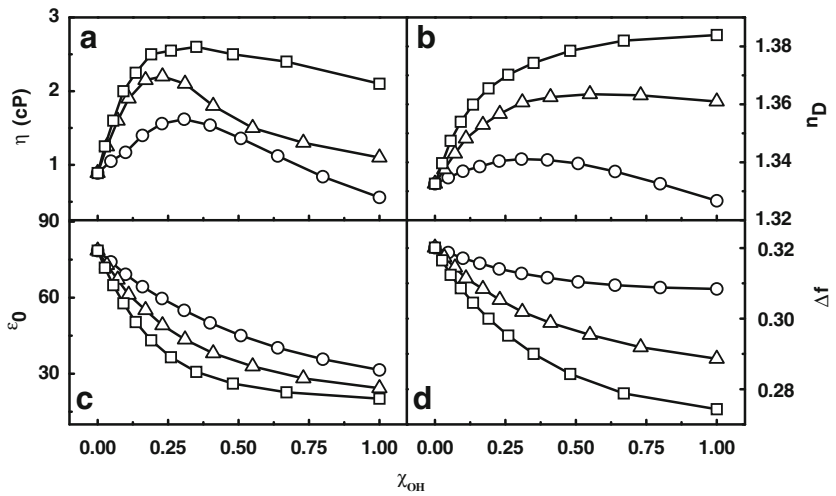

Fig. 3 Variation in physical properties of water-alcohol mixture at room temperature with alcohol mole fraction. Figs. **a**, **b**, **c** and **d** show the data for viscosity (η), refractive index (n_D), dielectric constant (ε_0) and orientation polarizability (Δf) for water–methanol (circle), water-ethanol (triangle) and water-1-propanol (square) solutions, respectively

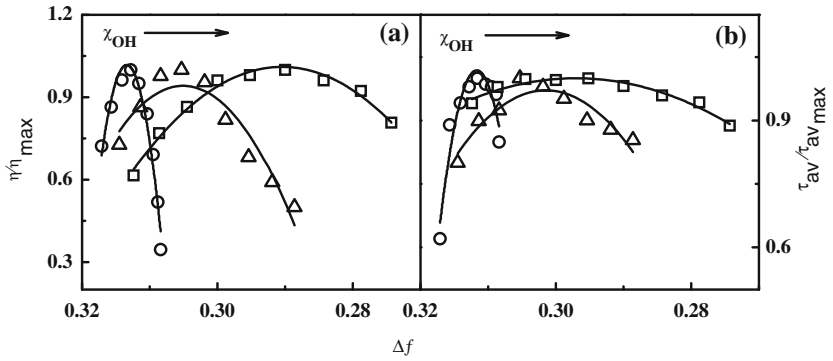

Fig. 4 Variation in (**a**) macroscopic viscosity (η) and (**b**) NCNP average lifetime (τ_{av}) as function of medium polarizability (Δf) at room temperature. Data shown in circle, triangle and square represents for methanol, ethanol and propanol solutions, respectively. Solid lines are fitting of data to Eq. 6

optimum fit and were fitted to Eq. 1 (see Fig. 2). All the results of the fitting like, amplitude, lifetime, average lifetime, and goodness of fitting (χ^2) are listed in Table 1. The average lifetime was calculated by using Eq. 2. The presence of multiple fluorescent states is most probably due to size heterogeneity of the fluorophores used in these studies. Their correlation with environmental parameters such as polarizability and viscosity discussed later.

Wang et al. [23] successfully established correlation between size of carbon nanodots, and fluorescence quantum yield, and lifetime through a series of investigations. The estimated lifetime ranged between ≈ 2 to 5 ns. Carbon nanoparticles (diameter ≈ 3–4 nm) prepared by microwave pyrolysis have shown luminescence lifetime ≈ 9 ns which was attributed to the radiative recombination nature of excitations [24]. Zhu et al. [34] further argued that there must be quantum confinement of emissive energy traps on the particle surface that allow red shift with increase in particle size, similar to those in quantum dots. Carbon dots with passivated surfaces have shown lifetimes in few nanoseconds region [25, 26]. Pan et al. [27] reported observation of pH, solvent, spin and excitation dependent blue photoluminescence from carbon nanoparticles prepared by pyrolysis of ethylene-diaminetetraacetic acid (EDTA) salts at low temperature. The lifetimes estimated for our systems (see Table 1) are comparable to the values reported in the literature cited above.

Addition of alcohol to water changes the physical parameters of the solutions considerably which is well documented in the literature [28–31] and Fig. 3 depicts is clearly. Solution viscosity (Fig. 3a) shows nonlinear change with the addition of increasing amount of alcohols with a maximum value occurring at $\chi_{OH} \approx 0.3$. The three alcohols followed similar trend. The refractive index and dielectric constant behavior for all alcohol solutions is shown in Fig. 3b and c. This data has been used to determine the Δf parameters for various solutions using Eq. 5 which is shown in Fig. 3d.

Fluorescence study of hydrogen bonded fluorephore, Rhodamine $3B^+$ was reported in water-ethanol binary solvents by Ferreira and Costa [32]. The Rhodamine $3B^+$ lifetime was observed to increase linearly from 1.49 ns to 2.25 ns as the solvent polarizability decreased, but the corresponding viscosity changes fallowed a nonlinear trend (consistent with the data shown in Fig. 3a with increasing ethanol mole fraction. Increasing alcohol chain length reduces solvent polarizability (see Fig. 3d). Thus, lifetime of the fluorephore should increase in general. We have used only three primary alcohols, as higher alcohols are immiscible with water, to show universal fluorescence behavior of NCNP in this limited set of three alcohol solutions. However, in our study of UV–vis absorption and PL, we show that alcohol chain length affects the fluorescence behavior of NCNP dispersed in selective alcohol solutions rather significantly. For example, UV–vis absorption spectra showed a very weak absorption band at 20% methanol, but for propanol strong absorption band was observed at same concentration. Average lifetime increased from 4.23 ns to 4.35 ns for methanol to propanol solvent. Lifetime data is presented in Table 1 indicates that though lifetime components did not vary following any specific trend in all solutions, but the average lifetime showed an identifiable trend similar to that of macroscopic viscosity (see Fig. 4). These features are summarized in Fig. 4 which is quite revealing.

The data was fitted to

$$X(\Delta f) = a_{OH} + b(\Delta f - \Delta f_{OH}) + c(\Delta f - \Delta f_{OH})^2 \qquad (6)$$

Where $X = \tau_{av}/\tau_{max}$ or η/η_{max} and the subscript OH represents corresponding value for alcohol. The fitting results are listed in Table 2.

Table 2 Results of the fitting of data in Fig. 4 to Eq. 6

Sample	Values for alcohols	b	c	χ^2
Methanol	η_{0H}=0.411	242	-2.42×10^4	0.91
	τ_{0H}=0.88	81	-1.22×10^4	0.90
	Δf_{OH}=0.305			
Ethanol	η_{0H}=0.43	62	-1.87×10^3	0.92
	τ_{0H}=0.816	22	-8.806×10^2	0.83
	Δf_{OH}=0.285			
Propanol	η_{0H}=0.80	25	-7.77×10^2	0.98
	τ_{0H}=0.89	10	-2.10×10^2	0.95
	Δf_{OH}=0.274			

The results clearly reveal that Eq. 6 describes the universal dependence of fluorescence lifetime and solution viscosity on medium polarity. In the past, the microscopic viscosity of complex liquids has been successfully probed by fluorophores using lifetime measurements. In this study, we show, even the macroscopic viscosity is amenable to such probing.

Conclusion

In summary, we have successfully used carbon nanoparticles as fluorophores to evaluate the fluorescence characteristics of alcohol solutions. The solutions were characterized through their polarity defined by polarizability. We have found that the fluorescence lifetime and solution viscosity could be described by an explicit quadratic function of solvent polarity. Such dependence has not been reported hitherto.

Acknowledgements Authors would like to thank AIRF, JNU for providing access to TRFS facility. PK thanks to University Grants Commission, Government of India for providing a research fellowship.

References

1. Onori G, Santucci A (1996) Dynamical and structural properties of water/alcohol mixtures. J Mol Liq 69:161–181
2. Cinelli S, Onori G, Santucci A (1999) Effect of 1-alcohols on micelle formation and protein Folding. Colloids and Surf A: Phys and Eng Aspects 160:3–8
3. Kresheck GC (1975) In: Franks F (ed) Water a comprehensive treatise, vol 4. Plenum Press, New York, pp 119–120
4. Varilly P, Patel AJ, Chandler D (2010) An improved coarse-grained model of solvation and the hydrophobic effect. J Chem Phys 134:074109–074115
5. Angelo MD, Onori G, Santucci A (1994) Self-association of monohydric alcohols in water: Compressibility and infrared absorption measurements. J Chem Phys 100:3107–3112
6. Laaksonen A, Kusalik PG, Svishchev IM (1997) Three-dimensional structure in water–methanol mixtures. J Phys Chem A 101:5910–5918
7. Patel SA, Brooks CL III (2005) Structure, thermodynamics, and liquid–vapor equilibrium of ethanol from molecular-dynamics simulations using nonadditive interactions. J Chem Phys 123:164502–164512
8. Biscay F, Ghoufi A, Malfreyt P (2011) Surface tension of water–alcohol mixtures from Monte Carlo simulations. J Chem Phys 134:044709–044710
9. Kaatze U, Pottel R, Schafer M (1989) Dielectric spectrum of dimethyl sulfoxide/water mixtures as a function of composition. J Phys Chem 93(14):5623–5627
10. Wang Y-M, Kamat PV, Patterson LK (1993) Aggregates of fullerene C60 and C70 formed at the gas-water interface and in DMSO/water mixed solvents, A spectral study. J Phys Chem 97(34):8793–8797
11. Arbeloa TL, Estévez MJT, Arbeloa FL, Aguirresacona IU, Arbeloa IL (1991) Luminescence properties of rhodamines in water/ethanol mixtures. J Lumin 48:400–404
12. Kohler G, Rechthaler K, Rotkiewicz K, Retti W (1996) Formation and stabilization of twisted intramolecular charge transfer states in binary mixed solvents. Chem Phys 207(1):85–101
13. Kumar P, Karmakar S, Bohidar HB (2008) Anomalous self-aggregation of carbon nanoparticles in polar, nonpolar, and binary solvents. J Phys Chem C 112(39):15113–15121
14. Kumar P, Bohidar HB (2010) Aqueous dispersion stability of multi-carbon nanoparticles in anionic, cationic, neutral, bile salt and pulmonary surfactant solutions. Colloids and Surf A: Phys and Eng Aspects 361:13–24
15. Bohidar HB, Kumar P (2010) Non-functionalized Carbon Nanoparticles having Fluorescence Characteristics, Method of Preparation Thereof, and their Use as Bioimaging and Solvent Sensing Agents. Indian Patent DEL/2184
16. Lakowicz JR (2002) Principles of Fluorescence Spectroscopy, 2nd edn. Kluwer Academic/Plenum, New York
17. Mataga N, Kubota T (1970) Macromolecular Interaction and electronic spectra. Mercel Dekker, New York, p 371
18. Amos AT, Burrows BL (1973) Solvent shift Effects on Electronic Spectra and Excited-State Dipole Moments and Polarizabilities In: Adv Quantum Chem Vol 7 pp 289–313
19. Von Lippert E (1957) Spektroskopische bistimmung des dipolmomentes aromatischer verbindungen im ersten angeregten singulettzu stand. Z Electrochem 61:962–975
20. Mataga N, Kaifu Y, Koizumi M (1956) Solvent effects upon fluorescence spectra and the dipole moments of excited molecules. Bull Chem Soc Jpn 29:465–470
21. Kimura Y, Sato T, Kaito C (2004) Production and structural characterization of carbon soot with narrow UV absorption feature. Carbon 42:33–38
22. De Heer WA, Ugarte D (1993) Carbon onions produced by heat treatment of carbon soot and their relation to the 217.5 nm interstellar absorption feature. Chem Phys Lett 207(4):480–486
23. Wang X, Cao L, Yang ST, Lu F, Meziani MJ, Tian L, Sun KW, Bloodgood MA, Sun YP (2010) Bandgap-like strong fluorescence in functionalized carbon nanoparticles. Angew Chem Int Ed 49:5310–5314
24. Zhu H, Wang X, Li Y, Wang Z, Yang F, Yang X (2009) Microwave synthesis of fluorescent carbon nanoparticles with electrochemiluminescence properties. Chem Com 34:5118–5120
25. Goncalves H, Esteves da Silva JCG (2010) Fluorescent carbon dots capped with PEG200 and mercaptosuccinic acid. J Fluores 20:1023–1028
26. Mao XJ, Zheng HZ, Long YJ, Du J, Hao JY, Wang LL, Zhou DB (2010) Study on the fluorescence characteristics of carbon dots. Spec Acta A: Mol Biomol Spec 75:553–557
27. Pan D, Zhang J, Li Z, Wu C, Yan X, Wu M (2010) Observation of pH-, solvent-, spin-, and excitation-dependent blue photoluminescence from carbon nanoparticles. Chem Com 46:3681–3683
28. Nagasawa Y, Nakagawa Y, Nagafuji A, Okada T, Miyasaka T (2005) The microscopic viscosity of water–alcohol binary solvents studied by ultrafast spectroscopy utilizing diffusive phenyl ring rotation of malachite green as a probe. J Mol Struct 735:217–223
29. Katti AM, Tarfulea NE, Hopper CJ, Kmiotek KR (2008) Prediction of viscosity-temperature-composition surfaces in a single expression for methanol–water and acetonitrile-water mixtures. J Chem Eng Data 53:2865–2872
30. Åkerlöf G (1932) Dielectric constants of some organic solvent-water mixtures at various temperatures. J Am Chem Soc 54:4125–4139
31. Wohlfarth Ch, Wohlfarth B, Binary Mixtures: Extended Data Lechner, MD (ed.) Springer Materials - The Landolt-Börnstein Database (http://www.springermaterials.com) doi:10.1007/10478514_8
32. Ferreira JAB, Costa SMB (2003) Non-Markovian effects in the radiationless decay of rhodamine $3B^{+}$ in water:ethanol mixture. Phys Chem Chem Phys 5:1064–1070